Universiteit Antwerpen

This item is the archived peer-reviewed author-version of:

A simplified model to assess the thermal performance of pavement solar collectors

Reference:
Ghalandari Mohammadtaher, Ceulemans David, Hasheminejad Navid, Guldentops Gert, Van den bergh Wim, Verhaert Ivan, Vuye Cedric.- A simplified model to assess the thermal performance of pavement solar collectors
Applied thermal engineering: design, processes, equipment, economics - ISSN 1873-5606 - 197(2021), 117400
Full text (Publisher's DOI): https://doi.org/10.1016/J.APPLTHERMALENG.2021.117400
To cite this reference: https://hdl.handle.net/10067/1799390151162165141

uantwerpen.be
Institutional repository IRUA

A simplified model to assess the thermal performance of pavement solar collectors

Taher Ghalandari*[,1], David Ceulemans[2], Navid Hasheminejad[1], Gert Guldentops[3], Wim Van den bergh[1], Ivan Verhaert[1], Cedric Vuye[1]

[1] Energy and Materials in Infrastructure and Buildings (EMIB) Research Group, Faculty of Applied Engineering, University of Antwerp, 2020 Antwerp, Belgium

[2] CoSys-Lab, Department of Electromechanics, Faculty of Applied Engineering, University of Antwerp, 2020 Antwerp, Belgium

[3] Simpson Gumpertz & Heger Inc. (SGH), 480 Totten Pond Rd, Waltham, MA 02451, United States

Abstract

The assessment of thermal performance and efficiency of the Pavement Solar Collector (PSC) systems is essential in designing such systems. In this paper, a simplified simulation model is developed to predict PSC's performance at the design stage. Due to its simplicity, accuracy, and extremely quick simulation run-time, the model output can be linked with other thermal models and renewable heat sources to apply real-time changes in the PSC systems and used in the automation of a PID-controller.

The output results show good compatibility between the predicted and simulated data, where the relative error values for model parametrization and validation are less than 0.21% and 0.5%. In terms of computational cost, a yearly long-term performance run time of the present model was simply 3 seconds (without parametrization), 300000 times faster than a FEM model for only one month.

A systematic sensitivity analysis on different design parameters shows that the efficiency index increases with an increase in pipe spacing, pipe embedment depth, and flow rate, while it decreases with an increase in the asphalt thermal conductivity in the wintertime. Also, the variation of the heat transfer coefficient UA* and correlation parameter k in different PSC configurations was established.

Keywords: Energy harvesting, Solar energy, Solar collector, Pavement Solar Collector (PSC), Asphalt pavement, Asphalt solar collector

Highlights

- A simplified simulation model based on energy flows and heat balance in Pavement Solar Collectors (PSC)
- A quick and accurate model to investigate the long-term thermal performance of PSCs in the design phase
- A large-scale PSC prototype was used to develop and validate the present model
- The model can interact with simulation environments, heat sources, and heat pump for real-time automation
- Systematic sensitivity analysis to identify the influence of design parameters on system performance

Abbreviations:

PSC, Pavement Solar Collector; UHI, Urban Heat Island; STES, Seasonal Thermal Energy Storage; FEM, Finite Element Method; LMTD, Logarithmic Mean Temperature Difference; NTU, Number of Transfer Units; CyPaTs, Cycle Pavement Technologies; HEAL, Heat Exchanging Asphalt Layer; GCHAP, Ground-Coupled Hydronic Asphalt Pavement.

---

* Correspondence to: Groenenborgerlaan 171, 2020 Antwerp, Belgium.
E-mail address: taher.ghalandari@uantwerpen.be (Taher Ghalandari).

1. Introduction

In recent years, researchers have shown an increased interest in renewable energy sources in order to provide clean and sustainable energy sources instead of fossil fuels. The demand for renewable energy sources directly results from the population explosion, urbanization, and environmental challenges. Solar energy is a proper substitute for fossil fuels, and its energy harvesting potential has been studied extensively in different engineering fields [1, 2]. The last two decades have seen a growing trend towards energy harvesting technologies from asphalt pavements. Energy extraction from asphalt pavement using Pavement Solar Collector (PSC) systems is one of the highly promising technologies due to their extensive availability in the roads, parking lots, airports, bicycle paths, etc., and great potential to absorb solar radiation [3].

The solar energy can be extracted on hot days by circulating a cooler fluid through the heat exchanger layer in the asphalt pavement structure. The heat exchanger layer can be constructed using a network of embedded pipes or a porous asphalt layer [4]. Although the PSC systems harvest low-temperature thermal energy, this energy can be used to provide domestic hot water, residential heating systems, and industrial applications [5, 6]. In addition to clean energy harvesting [5], PSCs can be employed to increase the asphalt pavement's service life, increase road safety [7, 8], and reduce environmental impacts [9, 10]. The PSCs harvest heat energy of the asphalt pavement and store it in a Seasonal Thermal Energy Storage (STES) (e.g., in a natural aquifer or using a man-made borehole thermal energy storage). This collected heat in the summer provides the required heat for de-icing or snow melting on the asphalt surface in wintertime. Hence, the STES systems form the thermal source of the heat pump during the winter period, while in the summertime, it acts as heat storage. It should be noted that the heat pump extracts the low-temperature heat from the STES to supply the PSC's heat source and can increase its temperature through a compression and expansion process if a higher inlet fluid temperature is required. The extraction of the absorbed solar radiation and moderating the asphalt temperature in winter by pumping the preserved heat can decrease the existence of pavement distresses such as top-down cracking, rutting, and fatigue cracking [11].

Recent research has led to a proliferation of studies that focus on the feasibility and performance of PSC systems, including small/lab-scale [12, 13] and large-scale set-ups [14, 15]. Although experimental works are necessary to have an understanding of the system performance, analytical or numerical simulation tools are also an indispensable part of the research studies on PSC systems. Due to the high cost of constructing experimental set-ups [11] to determine the sensitivity of design parameters and overall performance of the system, simulation tools are highly recommended to carry out parametric studies [16, 17]. Guldentops et al. [18] developed an FE-based experimentally validated modeling framework to predict the energy output of the PSC system with a high degree of accuracy. In addition to parametric analysis, the presented modeling framework can be used to improve the efficiency of the system in the design stage. Guldentops et al. [18] modeled the PSC system in full-scale 3D without any geometrical simplifications to perform a comprehensive and accurate evaluation of the system. However, the full-scale 3D finite element PSC models run into considerable computational run time. Mirzanamadi et al. [8, 19] proposed a hybrid 3D numerical model to simulate the anti-icing performance of the PSC systems. In this numerical model, a superposition principle is employed to separate the numerical simulation model into sub-models to employ linear equation systems and reduce the computation time. The proposed numerical model is developed in commercial FE software using the FEM technique and validated with experimental data. Several research studies implemented CFD models to simulate small/lab-scale and large-scale experimental PSC systems [15, 20, 21]. In addition to the development of an experimentally validated numerical model, Masoumi et al. [20] proposed an artificial neural network model to perform parametric studies on PSC systems. The proposed artificial neural network model is capable of simulating the PSC performance with compensating for the computationally intensive run time of the CFD model. However, the studies on simulation of PSCs may suffer from a significant error between model and experimental results [16] and computationally intensive run time [20]. Hence, a simple, yet comprehensive and accurate simulation tool is essential to study the thermal performance and efficiency of the PSC systems.

This paper introduces a new approach to investigate the thermal performance of the PSC systems. The presented simplified simulation model provides a reasonably accurate and extremely quick long-term simulation of the thermal behavior of the PSC system, as validated by comparing the output with a FE model. Due to its simplicity and quick run-time, this model can be implemented as a simulation tool in the initial design phase and feasibility assessment of a large-scale project. Due to its low computation cost and the focus on the thermo-hydronical behavior, the presented model can be linked or integrated into existing design software like HySopt [22], incorporated in novel design strategies for hybrid heating and cooling systems [23], and used within real-time model-based control or automation. Also, the model has the ability to interact with other simulation environments (e.g., Simulink) easily, which differentiates this model from other simulation tools. This study has two primary aims: (1) to provide an overview and framework of the proposed simulation approach, compared to a traditional FEM model as described in [18], and (2) to determine the long-term overall output of a large-scale PSC system.

This paper has been divided into five sections. The second section deals with the methodology used for this study, including governing energy balance equations in the PSCs and the description of the proposed simplified simulation model. Section three begins by laying out the experimental and numerical dimensions of the research and looks at how the experimentally validated modeling framework is implemented in this study. The fourth section presents the research findings, focusing on the three key themes; model parametrization, validation with experiment-based FEM models, and sensitivity analysis of the design parameters. Finally, the last section provides a summary of the main findings of the study and explores potential improvements for future studies.

2. Simulation Model Principle

In this section, first, the theoretical background of the energy balance of the PSC systems is discussed to provide an overview of the exchanged energy between flowing fluid and asphalt pavement. Second, a simplified simulation model is introduced, including its inputs, outputs, and working principle.

2.1. Energy Balance of PSC

In this study, a simulation model is developed based on the hydronic heat exchanger working principle, which provides a quick overview of the thermal performance of the PSC system with a reasonable degree of accuracy. To achieve this goal, the PSC should be investigated in terms of a low-temperature heat exchanger within a hydronic heating network. The simplified simulation model is developed based on the energy flows and the heat balance in the PSC system. Figure 1 shows a 2D schematic of the presented simulation model, including its heat flows and considered control volumes.

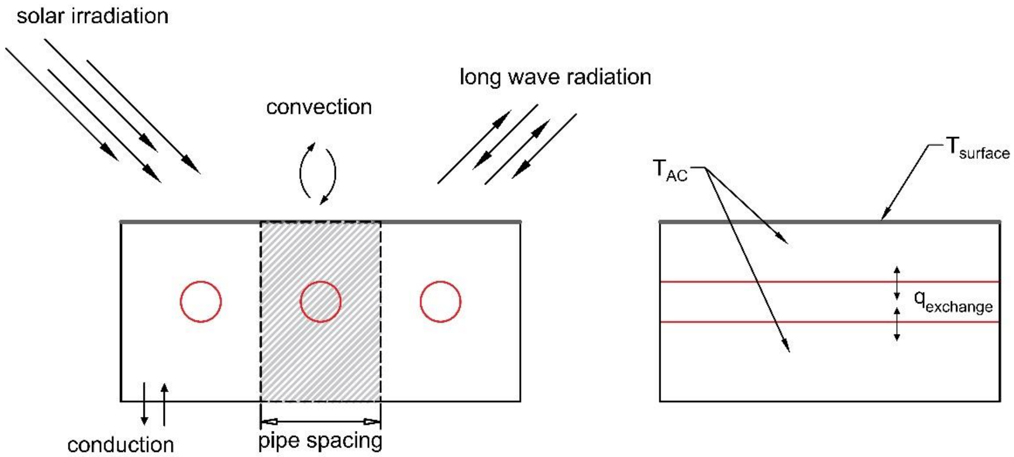

Figure 1. Schematic of cross-sections of the presented simulation model; (left) heat flow, (right) control volumes including asphalt surface, asphalt pavement, and circulating fluid

It should be noted that the shaded area in Figure 1 (left) is the subjected control volume for the heat exchange calculations. In the simplified simulation model, the PSC is subdivided into equally spaced (i.e., pipe spacing) parallel control volumes, representing similar control volumes. Therefore, it can be assumed that the horizontal heat flows are negligible, and the control volume exchanges heat with circulating water in PSC and with the environment mostly through the upper surface boundary.

The pavement surface is subjected to three heat transfer modes; solar radiation, convection, and conduction. An energy balance equation at the surface boundary of the asphalt pavement includes conduction, absorption and reflection of solar radiation, absorption and reflection of longwave radiation, emission of longwave radiation, and convection. The presented energy balance equation in this study does not include any form of precipitation heat transfers such as rainfall, snowmelt, latent snow heat, etc.

The total heat balance in the PSC that occurs between asphalt pavement layers, circulating fluid, and pavement surface can be calculated according to Eq. (1), where heat flow into the asphalt pavement has a positive value.

$$q_{heat\ balance} = q_{exchange} + q_{sw} + q_{lw} + q_{cv} + q_{cond} \quad (1)$$

In Eq. (1), $q_{heat\ balance}$ is the total heat balance in the PSC heat exchanger, $q_{exchange}$ is total heat transfer between asphalt pavement and fluid, q_{sw} is absorbed solar radiation, and q_{lw} is longwave radiation. Finally, q_{cv} and q_{cond} are the heat transfer values due to convection and conduction.

The incident, absorbed, and reflected solar radiation at the pavement surface are defined as the amount of solar radiation that impacts the pavement surface, solar shortwave radiation absorbed by the pavement surface, and reflected amount to the environment following the solar irradiance. The absorptivity of the asphalt surface determines the ratio of solar shortwave absorption and reflection on the pavement—the surface absorptivity of the asphalt changes between 0.7 and 0.93 [15, 24, 25].

The net amount of solar radiation absorbed by an asphalt pavement surface can be calculated as follows:

$$q_{sw} = \alpha I \quad (2)$$

where α (-) is the absorptivity of the asphalt surface, and I (W/m^2) is the total solar irradiation on the asphalt surface.

The longwave radiation that impacts on the asphalt surface consists of absorption of counter radiation and emission of longwave radiation. The absorptivity for the longwave radiation is assumed a constant since a grey behavior is a reasonable assumption within the longwave radiation spectrum. Besides, the asphalt pavement absorbs a certain amount of heat energy and radiates back into the environment at a specific wavelength. In the case of an asphalt pavement, the heat energy is exchanged with surrounding objects and air temperature in the environment, which is represented as the sky temperature T_{sky} in the literature.

Different models to calculate $T_{sky}$are available in the literature. These models are mainly based on dry-bulb temperature T_a, dew point temperature T_d, cloud cover N, and relative humidity RH. Another required parameter, the sky emissivity ε_{sky}, is described in In the model developed by Walton et al. [26, 27], as a function of both cloud cover and dew point temperature (Eqs. (6) and (7)).

$$q_{lw} = \varepsilon\sigma(T_{sky}^4 - T_{surface}^4) \tag{3}$$

$$T_{sky} = \left(\frac{R_i}{\sigma}\right)^{0.25} \tag{4}$$

$$R_i = \varepsilon_{sky}\sigma T_a^4 \tag{5}$$

$$\varepsilon_{sky} = \left[0.787 + 0.764 \cdot \ln(\frac{T_d}{273})\right] \cdot (1 + 0.0224N - 0.0035N^2 + 0.00028N^3) \tag{6}$$

$$T_d = \frac{B\left[log\left(\frac{RH}{100}\right) + \frac{CT_a}{B+T_a}\right]}{C - log\left(\frac{RH}{100}\right) - \frac{CT_a}{B+T_a}} \tag{7}$$

where ε (-) is the asphalt pavement emissivity, σ (W/m^2.K^4) is the Stefan-Boltzmann constant, T_{sky} (K) is sky temperature, $T_{surface}$ (K) is asphalt surface temperature, R_i (W/m^2) is horizontal infrared radiation intensity, ε_{sky} (-) is sky emissivity, T_a (°C) is dry-bulb temperature, T_d (°C) is dew point temperature, *N* (-) is the cloud cover factor, and RH (-) is the relative humidity. Also, *B* and *C* are constant coefficients equal to 243.04 and 17.625, respectively [18].

Based on Eq. (3)-(7), the surface temperature of the asphalt pavement is essential to calculate the heat transfer via longwave radiation. Obviously, the asphalt's surface temperature has a significant impact on the heat collection efficiency of the PSC systems.

Due to the temperature differences between the asphalt surface and flowing air, the convection mechanism should be investigated to calculate the heat transfer between the asphalt surface and air. Depending on the initiation of fluid motion, convection can be natural and/or forced. The asphalt pavement surface is exposed to solar radiation on sunny days that results in an increase in surface temperature due to its dark color compared to the temperature of the surrounding air. Hence, the presence of an airflow tends to cool down the pavement during hot days. The heat transfer of convection can be calculated using Eq. (8)-(11):

$$q_{cv} = h_{cv}(T_{surface} - T_a) \tag{8}$$

$$h_{cv} = h_n + h_f \tag{9}$$

$$h_n = \frac{9.482\,|\Delta T|^{\frac{1}{3}}}{7.283} \qquad if\ \Delta T < 0$$
$$h_n = \frac{1.810\,|\Delta T|^{\frac{1}{3}}}{1.382} \qquad if\ \Delta T > 0 \tag{10}$$

$$h_f = 5.11\,FF^{0.78} \tag{11}$$

Where h_n and h_f are natural and forced convection heat transfer coefficients, respectively, ΔT (°C) is the temperature difference between surface and dew point temperature, and FF (m/s) is the wind velocity.

The temperature gradient in asphalt pavement (between different layers) is responsible for the heat transfer by conduction mechanism. Since the heat transfer by conduction results from the temperature gradient, heat will be conducted downwards if the surface layer is warmer than the underlying layers. The opposite will occur if the underlying layers are warmer compared to the asphalt surface. The amount of conducted heat between different asphalt layers can be calculated using Fourier's law. However, the presented simplified model does not incorporate the conduction heat transfer between the asphalt layers. It considers the PSC asphalt layers as a single mass with a constant temperature all over the asphalt. The identical asphalt mass temperature can be explained since the temperature distribution of asphalt pavement in depth is almost linear [28]. This assumption helps us to simplify the heat transfer equations resulting in a faster model compared to time-consuming FE-based models. Hence, the heat energy exchange occurs only between the flowing fluid through the collector tubes and the mass of asphalt layers. For this reason, the heat transfer due to conduction q_{cond} is calculated only in the interface between subgrade and asphalt pavement, which resembles the heat loss or gain from underlying soil layers. This specific heat loss/gain can be calculated using Eq. (12):

$$q_{cond} = \frac{\lambda_{soil}}{d} \cdot (T_{AC} - T_{soil}) \tag{12}$$

with λ_{soil} (W/m.K) the thermal conductivity of the soil mass, d (m) the depth of soil interface from the asphalt surface where the temperature is considered as constant, T_{AC} (K) the temperature of asphalt concrete, and T_{soil} (K) the constant temperature of the soil at this interface. The average ground temperature for different months is assumed to be 10 °C at 10 m below the ground surface [29].

2.2. Description of the model principle

The simulation model consists of three main control volumes: asphalt surface, asphalt pavement (as a single mass), and circulating fluid (see Figure 1). Each of these individual control volumes is defined with a specific heat capacity and temperature. Pavement surface includes solar radiation and convection as the main external heat transfer mechanisms. The heat transfer among control volumes is due to water flow through pipes and boundary conditions of the asphalt surface. For the sake of simplification and reduction of the required computation time, the pavement layers are assumed as a single mass, in which the total heat capacity of the asphalt pavement is calculated using Eq. (13):

$$C_{AC} = \sum (c_{pi}\, \rho_i\, d_i)\, A \tag{13}$$

Where C_{AC} (J/K) is the total heat capacity of the asphalt pavement, c_{pi} is the specific heat of each layer (J/kg.K), ρ_i (kg/m^3) is the density of the layers, d_i (m) is the thickness of each layer in the asphalt pavement, and A is the area of the solar collector.

It should also be noted that a clear distinction has been made between asphalt surface and asphalt pavement and, consequently, their heat exchange values.

The amount of heat energy exchange in the PSC is calculated based on the temperature of the circulating fluid and asphalt pavement. During the operational phase of the PSC, static and dynamic scenarios are predicted. In the static scenario, fluid is stationary in the pipes and is not flowing through the pipe network. This scenario is considered to evaluate the energy balance of the PSC system in the intermittent operation mode during its idle time. The total heat transfer between asphalt pavement mass and fluid may be obtained by using Eq. (14) with the form of Newton's law of cooling:

$$q_{exchange} = U.A.(T_{water} - T_{AC}) \tag{14}$$

where U (W/m^2.K) is the heat transfer coefficient and T_{water} (K) is the temperature of water in the pipes.

However, when fluid is circulating through the pipe network (dynamic scenario), the heat energy balance is calculated based on the temperature difference between the asphalt pavement mass and fluid in different time steps. The amount of exchanged heat when the fluid is circulating through the pipes is calculated according to the Logarithmic Mean Temperature Difference (LMTD) method. The LMTD method is a simple approach to analyze, design, and calculate the performance of heat exchangers [30]. The efficient performance of heat exchangers is a key theme since it plays a prominent role in their energy consumption.

$$q_{exchange} = U.A.\Delta T_{LMTD} \tag{15}$$

where ΔT_{LMTD} (K) is referred to as the logarithmic mean temperature difference of the heat exchanger heat flows.

Since the LMTD requires iterative calculations to determine the outlet temperature, the Number of Transfer Units (NTU) method is used to obtain the outgoing water temperature from the PSC. The NTU method is based on the maximum potential of interchangeable heat energy between asphalt pavement and flowing fluid through the pipes to determine outlet water temperature within a quick and non-iterative approach. In this study, it is assumed that the temperature of the asphalt pavement does not fluctuate when the outlet water temperature is calculated. According to the material properties provided in Table 1, the calculated total heat capacity of the asphalt pavement using Eq. (13) is around 4.02e6. The heat capacity of the water in the pipes is calculated per mass flow rate circulating through the pipes (in the dynamic scenario) since the heat exchange happens between asphalt pavement and circulating water at specific time steps. Hence, the heat capacity ratio *Cr* between water and asphalt pavement results in approximately 8.31e-4 and is set to zero to simplify the equations in the NTU method. The heat transfer between asphalt pavement and flowing fluid can be calculated by Eqs. (16)-(21).

$$C_r = \frac{C_w}{C_{AC}} = 0 \tag{16}$$

$$NTU = \frac{U.A}{C_w} \tag{17}$$

$$\mathrm{E} = \frac{1 - exp\{-NTU[1 + C_r]\}}{1 + C_r} = 1 - exp(-NTU) \tag{18}$$

$$q_{max} = C_{water}\left(T_{w,i} - T_{AC}\right) \tag{19}$$

$$q_{\varepsilon-NTU} = \mathrm{E}q_{max} \tag{20}$$

$$q_{hydro,\varepsilon-NTU} = \dot{m}\, c_{p,w}\, (T_{w,i} - T_{w,o}) \tag{21}$$

In the equations above, C_r (-) is the heat capacity ratio, C_w (J/K) is the heat capacity of water, and E (-) is the heat exchanger effectiveness. Furthermore, q_{max} (W/s) is the maximum possible heat transfer rate, $q_{\varepsilon-NTU}$ (W/s) is the actual heat transfer rate, $q_{hydro,\varepsilon-NTU}$ (W/s) is the energy output (i.e., or input in wintertime) of the asphalt solar collector system, $\dot{m}$ (kg/s) is the rate of flow, $c_{p,w}$ (J/kg.K) is the specific heat capacity of water, $T_{w,o}$ (K) and $T_{w,i}$ (K) are the outlet and inlet water temperature of the PSC, respectively.

Having determined the net heat energy transfer in the PSC, the asphalt temperature is calculated for the next time step using Eq. (22):

$$T_{AC}^{j+1} = \frac{q_{heat\ balance}}{C_{AC}}.\Delta t + T_{AC}^{j} \tag{22}$$

Where T_{AC}^{j} (K) and T_{AC}^{j+1} (K) are the temperature of asphalt pavement for the current and next time step, and Δt (s) is the current time step.

The outgoing water temperature of PSC for the upcoming time step is calculated according to the maximum potential of interchangeable heat energy between asphalt pavement and flowing fluid principle using Eq.(23):

$$T_{w,o}^{j+1} = T_{w,i}^{j} - \frac{q_{hydro,\varepsilon-NTU}}{\dot{m}\, c_{p,w}} \tag{23}$$

Where $T_{w,o}^{j}$ (K) and $T_{w,o}^{j+1}$ (K) are the outlet water temperature from the PSC system for the current and next time step.

The aim of this study is to build a quick simulation model as an alternative to computationally costly FE models, without a trade-off over the accuracy of the output results. The outcome of the presented model is using only two parametrized variables to provide quick and reasonably accurate predictions of the PSC behavior. The PSCs' thermal performance, such as estimating the collector area and heat extraction capacity, plays an important role in their design perspective (i.e., integration within district heating or combination with other energy sources in a hydronic network). For this reason, a simple model with quick simulation time and accurate output provides an understanding of the thermal performance of the PSC systems, which can be useful for the feasibility study, the initial design, or even the use phase.

The input data for the model can be categorized into four main groups: 1) measurement or simulated data for the parametrization,2) physics of the PSC system, 3) material properties and constant values, and 4) weather data. Input parameters related to the physics of a PSC system include the total length of tubes, the collector area, pipe spacing, thickness of different asphalt layers, and depth of soil interface at constant soil temperature. Material properties and constant values are the input parameters for specifications of materials that are used in the PSC, such as the density of various asphalt layers, the specific heat capacity of asphalt layers, emissivity and absorption of asphalt pavement, asphalt boundary conditions (e.g., initial pavement and surface temperature), and properties of circulating fluid (i.e., water heat capacity, inlet mass flow, and inlet water temperature). As described in the previous subsection, weather data is essential to calculate the energy balance of the PSC systems. The weather data used in the model are dry-bulb temperature, wind velocity, direct and diffuse horizontal solar irradiation, relative humidity, and cloud cover. The meteorological data can be accessed using available software (e.g., Meteonorm[†]), online databases from the meteorological agencies, and in-situ measurement.

In the presented simulation model, the pavement layers are assumed as a single mass, with a constant temperature value within its depth. A correlation parameter (k) is introduced to correlate the asphalt pavement temperature in terms of the surface temperature. This correlation factor depends on the weather data used in the simulations.

$$T_{surface} = k.T_{AC} \tag{24}$$

Among the parameter values, the heat transfer coefficient U and the correlation parameter k are variables that dramatically influence the PSC system's thermal behavior. These two parameters represent the simultaneous influence of several parameters on the performance behavior of the PSC. Since the values of these two variables are unknown, they need to be determined for a specific PSC system. Hence, to predict the thermal behavior of a PSC system during a whole year using the proposed simplified simulation model, these parameters should be determined for only one month in cold seasons (autumn and winter) and one in warm seasons (spring and summer). Depending on the operation state of a PSC, Eqs. (14) or (15) is used to calculate the total heat transfer between asphalt pavement and circulating fluid. In these equations, the heat transfer coefficient U (W/m^2.K) is accompanied by the planar area of the solar collector A (m^2). Therefore, a new parameter of UA* (W/m.K) is introduced and used in the rest of this paper, where A^* (m) is the surface area of the asphalt solar collector per running meter of the embedded tube.

To be able to use the proposed simplified simulation model, the heat transfer coefficient and correlation parameters need to be 'parametrized' and determined for a specific PSC configuration. The parametrization process can be carried out using reference performance results (i.e., experimental or numerical simulations). The present study generated the reference results using experimental/numerical models from a large-scale PSC prototype at the University of Antwerp (see Section 3). The parametrization of the heat transfer coefficient and the correlation parameter is performed by achieving the minimum error difference between output results from experimental/numerical models and the simplified simulation model.

The introduced simplified simulation model has been developed based on the forward explicit Euler method. This model implemented the Euler method to calculate output results (i.e., surface temperature and outlet temperature of the PSC) of a specific time step based on the previous step. To perform the parametrization, the simplified simulation model needs to run with parametrized UA^* and k values and determine the heat energy transfer in the PSC using Eq. (1). Then, the surface temperature of the asphalt pavement and outlet temperature of the flowing fluid in the PSC system can be calculated. Next, the relative error between the simulation result and the presented simplified

[†] www.meteonorm.com

model is determined. As a result, the heat transfer coefficient and correlation parameter associated with the minimum relative error will be selected as parametrized *UA** and *k* values. The global optimization toolbox of MATLAB is implemented to find the optimum values for the *UA** and *k* that minimize the relative error (*RE*) function in Eq. (25).

$$RE = \left|\frac{Output_{\text{reference data}} - Output_{\text{simulation model}}}{Output_{\text{reference data}}}\right| \tag{25}$$

A step by step flowchart of the proposed simplified simulation model is given in Figure 2.

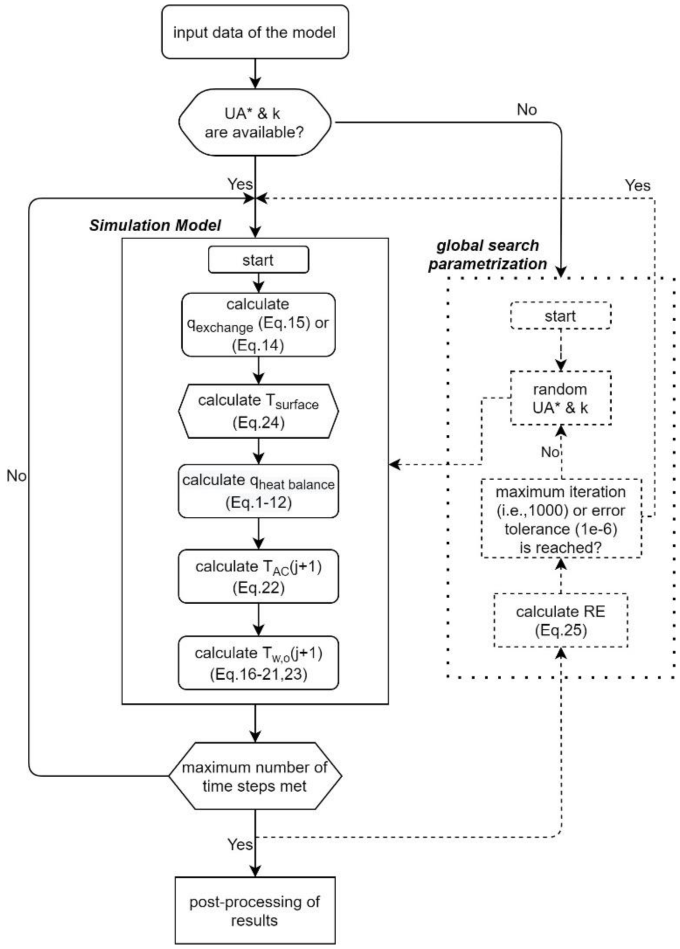

Figure 2. Flowchart of the simplified simulation model

3. Numerical Modelling Framework of a Large-scale Prototype

This section provides an overview of the validated numerical modeling framework that has been employed as input for the simplified simulation approach. In the first part, a short description is given of a large-scale prototype PSC used as a case study of a specific PSC. Then, an experimentally validated numerical framework is described, including geometrical parameters, assumptions, and necessary simplifications.

This study extended and implemented a recently developed finite element (FE) modeling framework. The modeling framework has been validated with experimental results and showed a good agreement in terms of outlet fluid temperature and surface temperature of asphalt pavement [18]. The FE models are simulated in 3D to provide a comprehensive evaluation of the PSC system. It should be noted that the simulated models are based on a large-scale research PSC prototype that was constructed at the University of Antwerp [31].

The Cycle Pavement Technologies (CyPaTs) project implemented five innovative technologies within the sustainable asphalt pavement research field. The CyPaTs was constructed in 2017 in a bicycle path next to the Groenenborger campus at the University of Antwerp. A large-scale PSC is one of the five technologies in the CyPaTs project that were constructed as a demonstration project for the road construction sector and to be used for several research projects. For more details on the project description, refer to [31-34]. In the following paragraphs, the information about the Heat Exchanging Asphalt Layer (HEAL) project relevant to this study is presented.

The HEAL system was constructed in a total area of approximately 65 m^2. The project also includes reference sections (without HEAL) for the comparison of the results between HEAL and reference sections. The HEAL was placed in four independent heat exchange sections, with 8.5 m x 1 m dimension each, which makes it around 30 m^2 of the net area of the system (Figure 3). The asphalt pavement has a total of 12 cm thickness, placed on a 20 cm foundation layer from unbound materials. Details of the asphalt pavement specifications and the estimated thermal properties used in the FEM simulations are presented in Table 1.

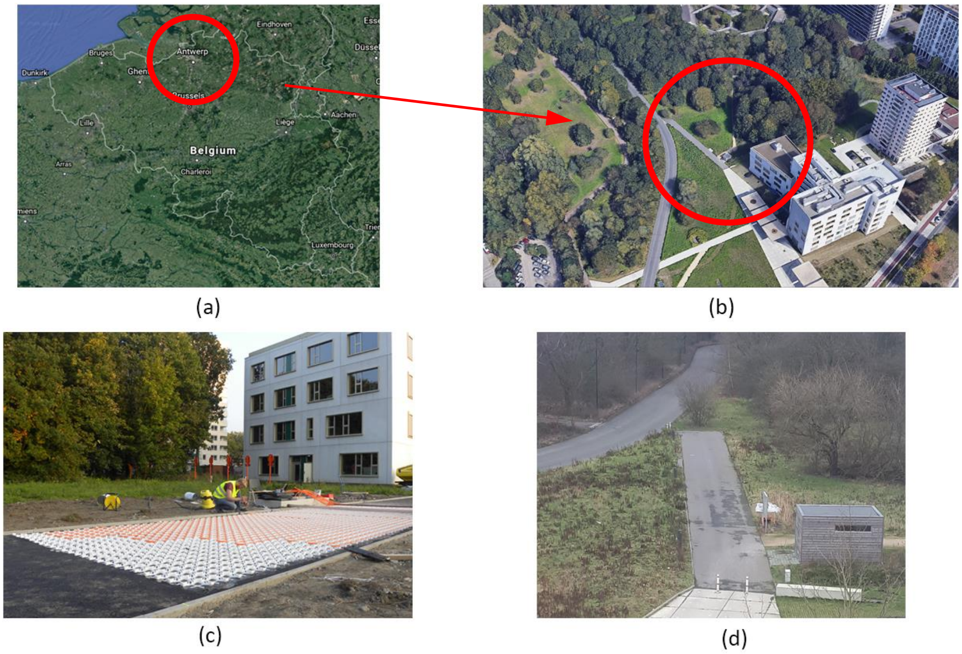

Figure 3. HEAL prototype (a) Location of the University of Antwerp in Belgium (b) Aerial view from HEAL prototype at campus Groenenborger (c) construction stage (d) post-construction and operational view of the project

Table 1. Material and thermal properties used in the simulations

Material	**Layer thickness (cm)**	**Thermal conductivity (W/m.K)**		**Density (kg/m^3)**	**Heat capacity (J/kg.K)**
FEM/present model	FEM & simplified model	FEM	simplified model	FEM & simplified model	FEM & simplified model
Asphalt pavement [18] a. Top layer b. Collector layer c. Base layer	 a. 3 b. 4 c. 5	1	-	2400	1000
Compacted Aggregates	20	0.505	-	1580	850
Soil [30]	2500	0.75	-	2000	850
Polyethylene pipe [30]	-	0.45	-	940	1900

The polyethylene pipes are arrayed in a serpentine configuration within the heat exchange layer, embedded (P_d = 4.5 cm) from the surface and with a (P_s = 15 cm) center to center pipe distance (Figure 4). The polyethylene pipe used in the prototype has a (D_{out} = 20 mm) outer and (D_{in} = 13 mm) inner diameter, respectively. The length and width of the PSC system for one section are (L = 8.5 m), and (W = 1.0 m). The network of polyethylene pipes is supported by a reinforcing grid, as developed by the Dutch contractor Ooms [35, 36], to support and protect the pipes from potential damages caused by heavy loads during and after construction. However, the reinforcing grid has not been modeled in the thermal simulations of the present study. The pipe networks were installed in four independent sections, each with a length of 50 m resulting in 200 m total length of embedded pipes. Furthermore, each heat exchanger section can be activated stand-alone or in combination with other sections, which enables the PSC system to perform different configuration scenarios such as heating the pavement partially or using the entire system. In this study, due to the high computational cost of the 3D simulation model, only one section of the PSC has been simulated (Figure 4, (a)). However, this is not in conflict with the aim of the present paper since it is assumed that each heat exchanger section can be solved separately, and the overall performance of the system can be calculated by adding up the outputs of different sections.

A 3D full-scale model of the large-scale PSC has been developed in COMSOL Multiphysics to simulate the thermal performance of the system (Figure 4, (b)-(d)). Developing a full-scale model was necessary to avoid thin wall assumptions and geometrical simplifications. In order to avoid unwanted convergence issues, the soil layer under the compacted aggregates is extended as 2.5 m in the simulations, resulting in a total height of 3.0 m for the FE model.

The COMSOL Multiphysics software was used to develop and solve the 3D numerical models using the Finite Element Method (FEM). The simulations were performed for a laminar flow regime, and split into two separate sub-problems to achieve an uncoupled thermal problem. This assumption results in a non-variable flow field in the entire model during the total run-time that effectively reduces computational time. For the thermal boundary conditions of the FEM models, the asphalt surface is exposed to solar radiation, ambient temperature, and convective heat flux. The inlet temperature of the fluid is set to a constant value. The rest of the boundaries are thermally insulated (adiabatic). For the laminar flow, a constant fluid flow was assigned at the inlet boundary. Furthermore, at the pipe wall, a no-slip boundary condition is selected. The FE model has a total of 128480 elements, where a grid refinement study confirmed its acceptable sensitivity. For the time-dependent solver, the calculation time-step of the FE models was set to 1800 s. Hence, a full month simulation run time for a model was approximately 22 hours, using a dedicated computer with the following specifications; 64.0 GB RAM, Intel(R) Core(TM) i9-9900K CPU@3.60 GHz processor, and an NVIDIA GeForce RTX 2070 GPU. For more details about the numerical simulation model of the PSC system, please refer to [18, 31].

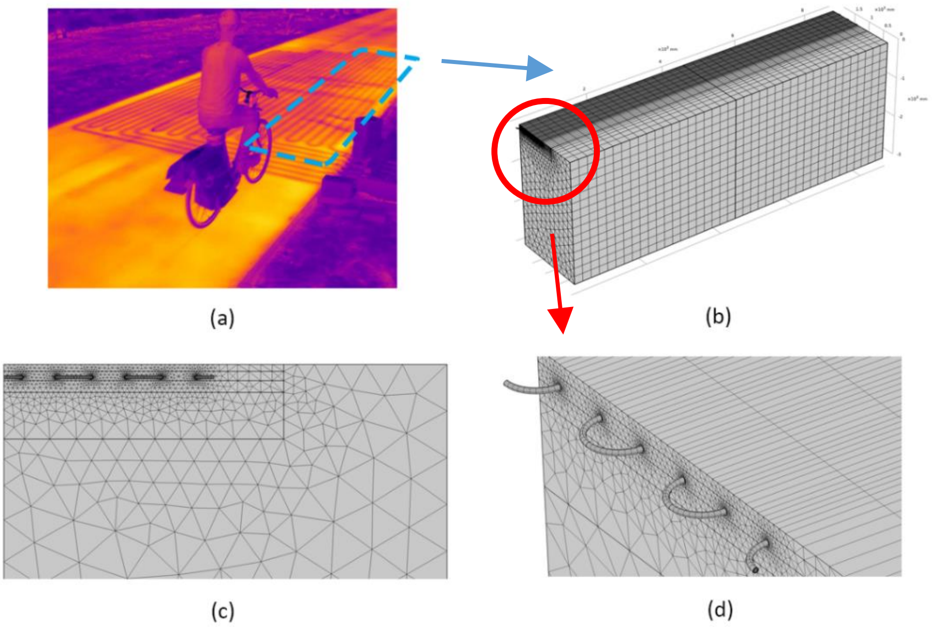

Figure 4. PSC simulation model (a) infrared photo from pipe sets (b) Full-scale 3D model (c) detailed front view of the model's mesh (d) detailed view of the optimized mesh of the model

4. Validation with an experiment-based FEM model

4.1. Model parametrization

As discussed in Section 2, to evaluate the PSC system's thermal performance in an entire calendar year using the simplified simulation model, the *UA** and *k* variables should be parametrized. As shown in the simplified simulation model flowchart (Figure 2), these two variables are identified through a global search optimization process, where realistic upper and lower boundaries (e.g., greater than zero) are assigned to the *UA** and *k* parameters in the optimization algorithm. In the parametrization procedure, a calendar year is divided into cold and warm months (i.e., April-September as warm months). A representative month from warm/cold months is first selected to obtain *UA** and *k* variables and next, and the corresponding parametrized values are used for the rest of the months in the same warm/cold category. In this section, the parametrization steps are discussed for the PSC prototype, using the weather data of the year 2018 for the simulation models. Based on the meteorological data of the selected location (Antwerp, Belgium), January and June were selected as the representative months for the parametrization of cold and warm seasons. A series of simulations have been performed to evaluate the most favorable reference months in the warm/cold grouping for the parametrization. In Table 2, first, a selected month has been parametrized, and then the output *UA** and *k* values were implemented in the simplified simulation model to provide the total (i.e., the cumulative error of all time steps) and mean relative error (i.e., total error divided by the number of time steps) of the selected month. For example, in June, the parametrized *UA** and *k* used for simplified simulation resulted in a total of RE 4.4256% and 2.8591% for the outlet temperature of the system for July and September, respectively. The study resulted in a very marginal difference in the total and relative error for various months as the representative reference for parametrization. For the sake of validation, February and December are selected as cold months, while July and September are chosen as warm months.

Table 2. The parametrization sensitivity for reference month in the warm season

Months	**June**		**July**		**September**		**parametrized values**	
	total RE	mean RE	total RE	mean RE	total RE	mean RE	UA*	k
June	-		3.8641	0.0027	3.1228	0.0022	1.668	0.965
July	4.4256	0.0030	-		4.2343	0.0028	1.814	1.017
September	2.8591	0.0020	3.1100	0.0022	-		1.829	0.986

The parametrization can be done for more months to increase the accuracy of the model. However, since the experimental data or numerical simulations are either costly or computationally intensive, providing data for one representative month for cold and warm seasons is suggested. Figure 5 provides an overview of the hourly dry-bulb temperature during the studied months in 2018 for the city of Antwerp.

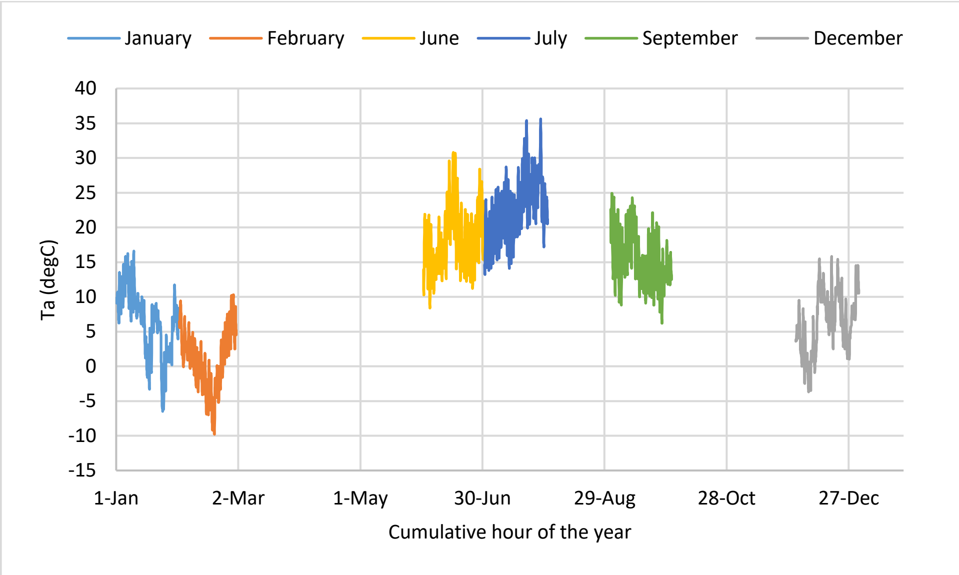

Figure 5. The hourly dry-bulb temperature of selected summer and winter months for simulation, Antwerp, 2018 (from Meteonorm software)

The parametrization of *UA** and *k* values for January resulted in 1.787 (W/m.K) and 1.084 (-), respectively. The same parametrization procedure resulted in *UA** and *k* equal to 1.668 (W/m.K) and 0.965 (-) for June. As mentioned previously in Eq.(1), a heat flow into the asphalt pavement is considered as a positive value. Since the *UA** factor represents the amount of heat exchange between asphalt and water regardless of heat flow direction, the resulted *UA** was different for various cold/warm months. Hence, the magnitude of *UA** does not characterize a distinct feature related to the parametrized month or season. It is noteworthy mentioning that the quantity of the *UA** value is a function of both thermophysical properties of asphalt pavement and operational conditions (e.g. weather data). The *UA** value is mainly influenced by the amount of heat exchange between asphalt and water, however, since *UA** and *k* variables are parametrized simultaneously, both parameters mutually impact to achieve the minimum RE in the optimization algorithm (Figure 2). Thus, the operational conditions impact temperature surface (i.e., *k* value), heat balance equation, outlet water temperature, and consequently minimum RE of the algorithm. Figure 6 shows the comparison of outlet temperature of the PSC predicted by both the FE model and the simplified simulation approach. It can be seen that the introduced simplified approach can simulate the thermal performance of the PSC system with a high degree of accuracy. To be able to compare the results from the two models more in detail, the relative error of the predicted outlet temperature with respect to the FE model (i.e., as a relatively accurate result reference) is calculated. The comparison of outlet water temperature from the two models and their corresponding relative errors for the representative month is presented in Figure 6. According to Figure 6 (b), the average RE (%) for January and June is 0.076 and 0.21, while the RE stays below 1% at all time steps. Although the average RE values indicate a better agreement between the models for January compared to June, to compare the RE more effectively, total RE is divided to the PSC's average outlet temperature (of all steps) that leads to 13.75 (1/K) and 13.81 (1/K) for January and June, respectively. Even though there are some error peaks in June, the total RE to average outlet temperature ratio shows that the presented model is able to parametrize both months with a good degree of accuracy.

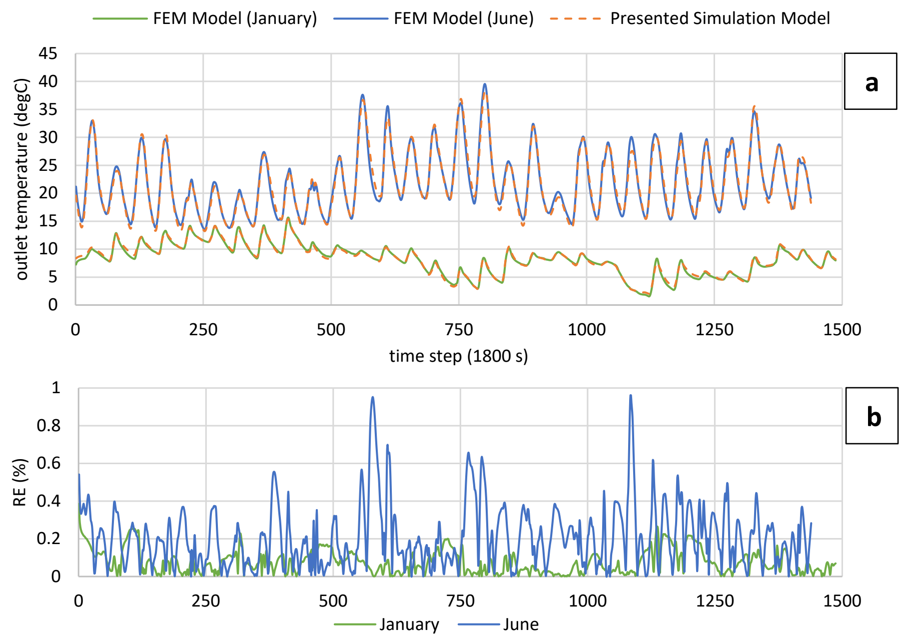

Figure 6. Comparison of results from the numerical models (FEM) vs. presented model; (a) outlet temperature of PSC, (b) the relative errors

4.2. Model verification

In this section, the output results of the experiment-based FEM simulations are compared with the presented simplified simulation model. To this end, the parametrized values of *UA** and *k* for cold and warm seasons are used to simulate the performance of a large-scale PSC system for an entire year.

In the first phase, the simplified simulation model is used to predict the seasonal performance of the PSC system. For the warm months, the parametrized heat transfer coefficient and correlation parameter values from June are implemented into the simplified simulation model. The predicted outlet temperatures from the PSC system from April 1^{st} until September 30^{th} are given in Figure 7. In order to validate the accuracy of the model, two different months from warm seasons (July and September) are selected, simulated in the FE model, and their results are compared with the presented model. Figure 7 shows good compatibility for the predicted output and experimental/numerical FE model. The relative error values in the two selected months for validation are less than 1 percent for almost all calculated time steps.

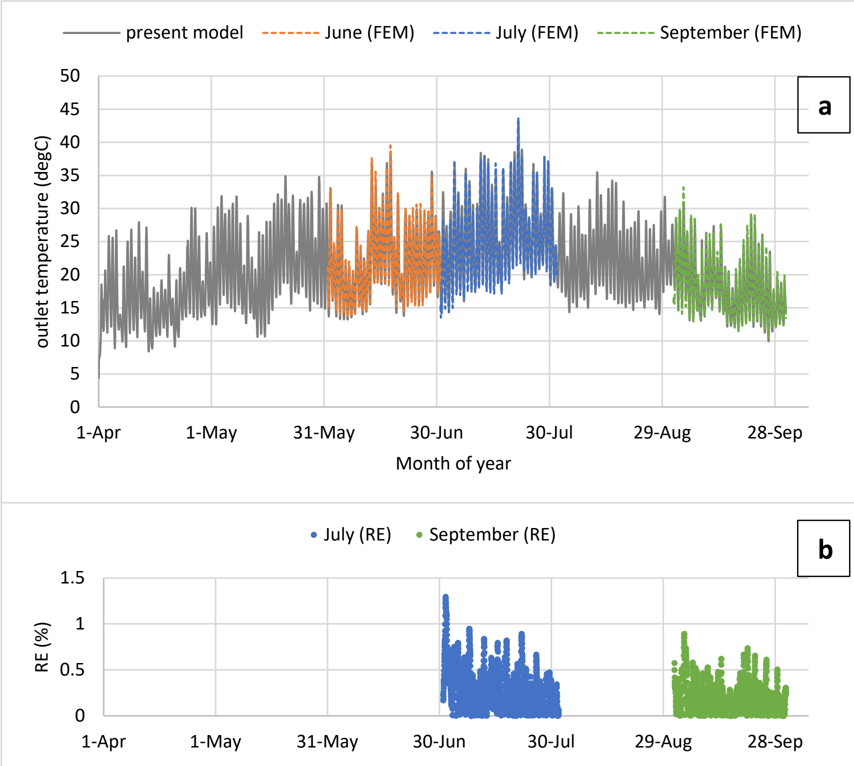

Figure 7. Comparison of results in warm months; (a) outlet temperature FEM and present model (b) REs for validated months

The same validation process has been performed for the cold season, taking December and February as the validation benchmarks. Using the parametrized values of *UA** and *k* parameters from January, the simplified simulation model presents outlet temperatures of the PSC system from October 1st until December 31st and January 1st to March 31st (Figure 8 (a)). Furthermore, the relative error values for the validated months are presented in Figure 8 (b), where the relative error is mainly around 0.2% and reaches a maximum of 0.5%.

Finally, the output power of the PSC system (at a time step of 1800 s) has been calculated using the simplified simulation model using the weather data of the year 2018 for Antwerp, Belgium (Figure 9 (a)). The positive output power value is related to energy harvesting, while a negative output power is associated with heat injection into the PSC. Figure 9 (a) indicates that the output power (approximately) from January 1st until April 1st and mid-September to December 31st is negative. The histogram of the output power for the PSC system is given in (Figure 9 (b)). The histogram shows that the concentration of power output of the system is in the range of (-500,-100). The cumulative output power of the system is calculated around 172 kW which shows that the PSC system is not only able to provide sufficient power for its use, but also it harvests low-temperature thermal energy from the asphalt pavement.

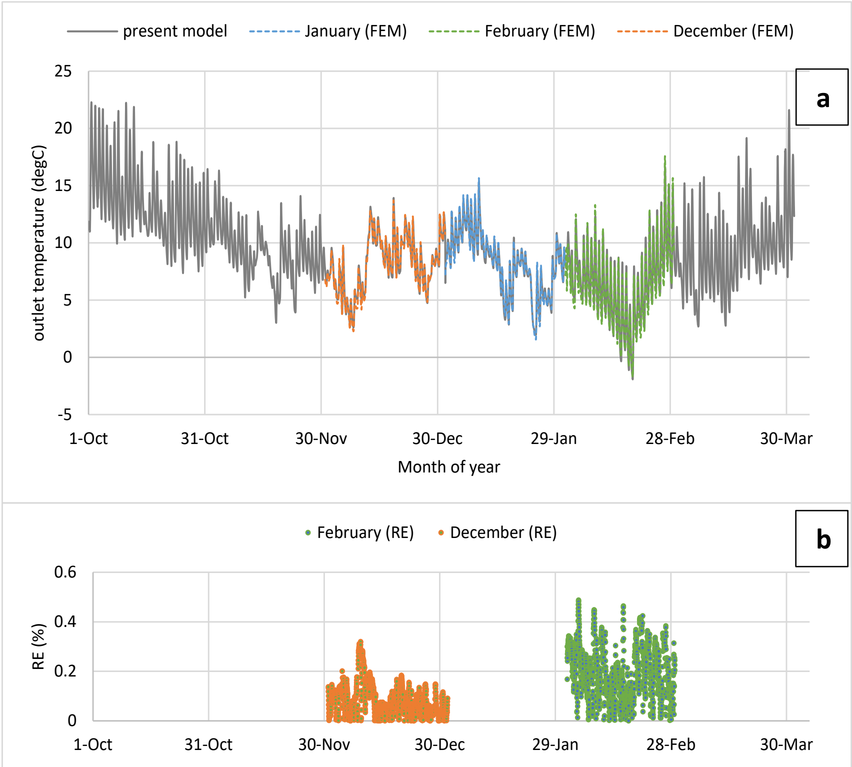

Figure 8. Comparison of results in cold months; (a) outlet temperature FEM and present model (b) REs for validated months

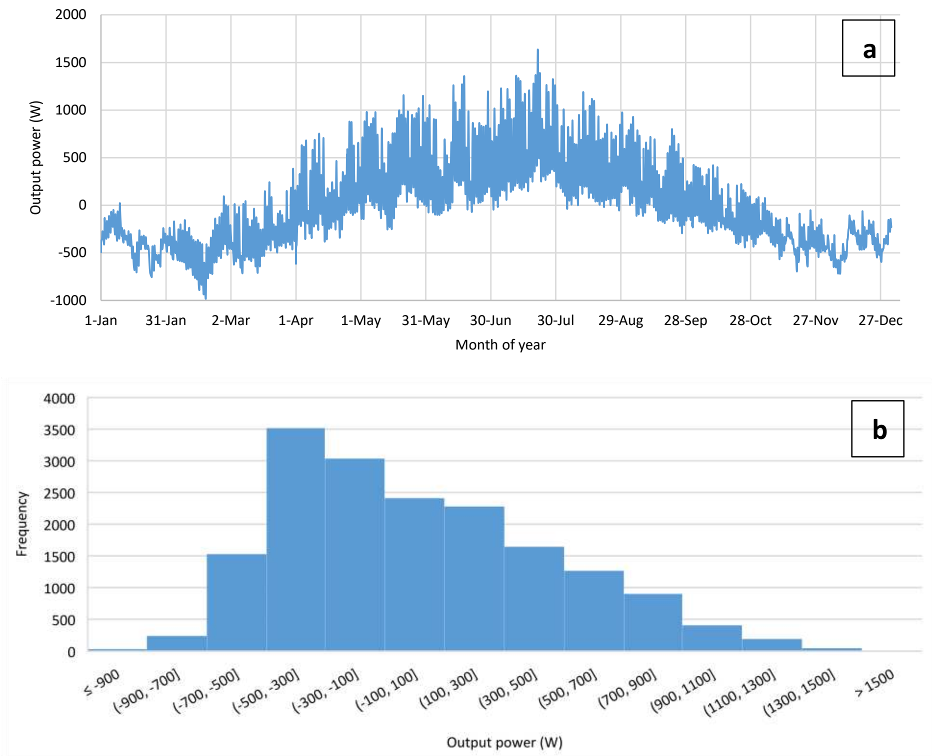

Figure 9. Long-term performance of the PSC system using the presented model (a) power output of the system (b) histogram of the output power

The simulation run time for the long-term performance over the calendar year of 2018 was only 3 s. The run time for the presented simplified simulation model is dramatically shorter than for the FEM simulation (approximately 22 hours for a month).

Due to its simplicity, accuracy, and extremely short simulation run-time, the presented model could be used to interact with other simulation environments (e.g., Simulink) or to perform the simulations for the real-time automation in a PID-controller. Also, using the interaction ability, the output of the presented model (i.e., outlet temperature) can be a direct input for other thermal models (e.g., a heat pump). Ground-Coupled Hydronic Asphalt Pavement (GCHAP) systems are mainly constructed to heat airport aprons, aircraft parking, and terminal buildings. In these hybrid PSC systems, the GCHAP is linked to a seasonal heat storage or an aquifer to keep the temperature balance between pavement and the circulating fluid. Also, the PSC systems are mainly programmed to operate continuously or intermittently, depending on the project need. A control system is used to automate the PSC and to activate in certain weather conditions (e.g., minimum air temperature or precipitation) or predetermined settings (e.g., minimum or maximum asphalt surface temperature). Therefore, the link between an accurate and quick simulation tool and other renewable heat sources is important to be able to monitor and update the control system in different operation modes.

4.3. Sensitivity Analysis

In this section, the sensitivity analysis has been performed on the design, material and flow parameters of a PSC to provide an overview of its performance variation. In this study, pipe spacing, pipe embedment depth, flow rate, and asphalt conductivity are investigated for sensitivity analysis.

For this reason, different individual FE models were developed for these parameters, and their output results have been used for parametrization and comparison of *UA** and *k* values in different cases. The FE models have been simulated for January 2018 using the meteorological data of the city of Antwerp. The sensitivity analysis aims to identify the influence of different design and model parameters and finding the impact of parameter changes on the heat transfer coefficient *UA** and the correlation parameter *k* in different PSC system configurations.

Several studies showed the impact of system parameters on the energy harvesting and snow melting performance of the PSC systems. Pipe spacing, embedment depth, asphalt thermal properties, flow rate, and pipe diameter are the most influential parameters on the system performance [2, 8, 25, 37]. This paper does not necessarily aim to optimize the system parameters, however, it sheds light on the output efficiency of the asphalt solar collector systems and related heat transfer coefficient and correlation parameter. The efficiency index (η) is defined, in Eq. (26), as the ratio between the energy input or output and the solar insolation on the asphalt surface (q_{sw}). The input and output energy refers to the injected heat (in winter) and extracted heat (in summer) within the PSC system. These input and output energy values ($q_{hydro,\varepsilon-NTU}$) are calculated according to the simplified simulation model using Eq. (21).

$$\eta = \frac{q_{hydro,\varepsilon-NTU}}{q_{sw}} \times 100 \tag{26}$$

Pipe embedment depth is one of the most influential design parameters on the thermal performance of PSC systems. Although a pipe network closer to the asphalt surface can be beneficial from an energy harvesting point of view, it should be deep enough to avoid potential damages due to excessive structural loads and required re-paving of the surface layer. Table 3 shows the effect of changing pipe embedment depth on the heat transfer coefficient, correlation parameter, and efficiency index. Based on Table 3, the heat transfer coefficient decreases around 39% when increasing the pipe depth from 35 to 90 mm. This drop in the heat transfer coefficient brings about a 15% increase in the PSC efficiency index (i.e., less heat injection required) since it is the main parameter to calculate the heat exchange between fluid and asphalt pavement. According to the definition in Eq. (26), the efficiency index is a positive value in the summertime due to solar energy extraction and negative in the wintertime because of heat injection to the system. Hence, relatively large efficiency index values in the wintertime can result from high injected heat and/or a low amount of solar insolation on the asphalt surface. According to the collected meteorological data for the selected location (Antwerp, Belgium), the amount of solar irradiation in January 2018 was low, resulting in a high (and negative) efficiency index (Table 3 and Figure 10).

As mentioned before, the sensitivity analysis has been performed for January 2018. Since the parameter *k* depends mainly on weather parameters, it was expected that it would not change for sensitivity studies in January. Hence, to demonstrate to what extent and how the efficiency index, *UA**, and *k* values change in a cold and warm month, we explored the variation of these parameters in different pipe depths (Table 3, right). With the increase of pipe embedment depth, the efficiency index and *UA** values decrease both in the cold and warm seasons. The *UA** is the most sensitive parameter for change of pipe depth in both cold and warm months, decreasing by 39% in January and 58% in June, respectively. The efficiency index reached the same variation for both January and June, by 15%. The *k* parameter is almost the same in January, while it decreases from 0.966 to 0.839 in June. This shows that the parameter *k* does not necessarily depend on the weather conditions. In addition to the sensitivity analysis results given in Table 3, a trend line of *UA** and efficiency values are provided in Figure 10. The R-squared values (around 0.98) given in Figure 10 (a) show a good linear correlation between the variation of pipe depth in the PSC system and *UA** and efficiency index.

pipe depth	UA* (W/m.K)	k (-)	η (%)
35	1.944	1.083	-213.78
45	1.759	1.086	-207.96
70	1.385	1.094	-193.00
90	1.188	1.090	-182.11

Month	pipe depth	UA* (W/m.K)	k (-)	η (%)
January	35	1.944	1.084	-213.78
	90	1.188	1.091	-182.11
June	35	1.734	0.966	25.30
	90	0.729	0.839	21.50

Table 3. Sensitivity analysis of pipe depth for efficiency index, UA* and k values (left) for January, (right) parameter change in January and June

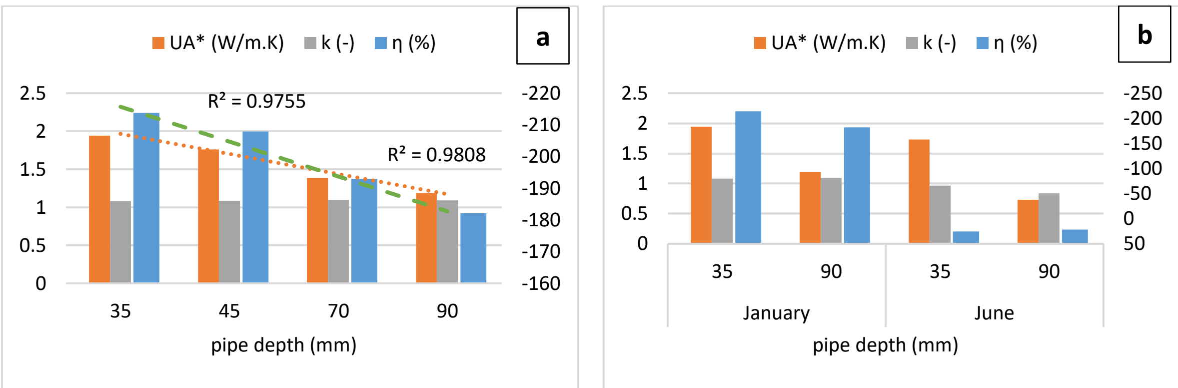

Figure 10. Parameter sensitivity: a) pipe depth sensitivity in January b) parameter change comparison in January and June for UA* and k (left axis), and efficiency index (right axis)

Another critical design parameter is the pipe spacing, which significantly affects the PSC systems' (long-term) thermal performance. For a similar PSC project size (same surface area), decreasing the pipe spacing will increase the total length of the pipe as well, which also impacts the system performance. As represented in Table 4, the *UA** value decreases dramatically from spacing 75 to 150 mm. However, the *UA** almost reaches a plateau by widening the spacing from 150 to 300 mm. In order to clarify the effect of pipe spacing variation on system performance, efficiency indices have been calculated and provided for different cases in Table 4 as well. The efficiency index increases by 38.9% from 254% to 155%, with a spacing equal to 75 and 300 mm.

Next, the parametric study has been done for different flow rates F_R= 10, 20, 30, 40, 50 (L/h) in the laminar flow regime. Simulation results show that the *UA** parameter decreases with the increase of flow rate, leading to a drop of the *UA** value by 61% when increasing the flow rate from 10 to 50 (L/h) (Table 4). Because simulations have been performed within a cold month (January), the output energy can be better explained by the amount of injected heat energy to the system. Hence, it can be summarized that increasing flow rate (in laminar regime limits) results in a decrease in heat exchange between circulating fluid and asphalt pavement.

Parameter	values	UA* (W/m.K)	k (-)	η (%)
pipe spacing (mm)	75	3.391	1.100	-254.27
	150	1.761	1.071	-207.96
	300	1.838	1.094	-155.38
flow rate (L/h)	10	4.560	1.091	-315.88
	20	3.369	1.094	-296.64
	30	2.212	1.084	-267.38
	40	1.982	1.086	-239.01
	50	1.759	1.086	-208.06
thermal conductivity (W/m.K)	1	1.759	1.086	-207.96
	1.5	2.769	1.069	-230.99
	2	3.761	1.063	-240.04
	2.5	6.121	1.060	-246.01

Table 4. Sensitivity analysis of pipe spacing, flow rate, and asphalt thermal conductivity for efficiency index, UA* and k values for January

Lastly, it has been previously shown in the literature that the increase of asphalt pavement thermal conductivity results in a more effective thermal energy harvesting [18]. The effect of asphalt thermal conductivity variation on *UA** and *k* parameters is provided in Table 4. Due to asphalt thermal conductivity variation from 1 to 2.5 (W/m.K) [18], the heat transfer coefficient value increases almost 2.5 times. This resulted in a decrease of the efficiency index by 18.5%, from 207% to 246%.

5. Conclusions

Pavement Solar Collector (PSC) systems have shown promising potential in harvesting solar energy from an asphalt pavement in the roads, parking lots, airports, and bicycle paths. The asphalt pavement can be cooled down by circulating a cool(er) fluid in summer to harvest solar heat for domestic and industrial applications. To understand and optimize different aspects of PSCs (i.e., design or performance), simulation tools can provide valuable information. Although several analytical and numerical simulation tools were developed to predict the behavior of the PSCs, their accuracy and computational cost can be questioned.

This paper introduces a quick and accurate simulation tool to investigate the long-term thermal performance and efficiency of the PSC systems. The presented simplified model simulates the PSC system as a low-temperature heat exchanger that is developed based on the energy flows and the heat balance in a PSC system. An experimentally validated modeling framework and a large-scale PSC prototype were employed to develop and validate the simplified simulation model.

The model can perform the simulations for real-time automation in a PID-controller and interact with other simulation environments (e.g., Simulink) due to its simplicity, accuracy, and extremely quick simulation run-time. Also, the output of the simulation model can be linked to other thermal models (e.g., heat pump) and renewable heat sources in order to monitor and adapt necessary real-time changes in the PSC system, such as activating it in certain weather conditions or programmed settings.

Comparing the output results (i.e., the outlet temperature of the system) provides a good agreement between the simplified simulation model and the employed FE model. The calculated average RE for parametrization is 0.076% and 0.21% for cold and warm months. Also, a thorough analysis of the most favorable reference warm/cold month for the parametrization revealed that the presented model is able to parametrize both seasons within a good degree of accuracy.

The relative error values from validation simulation data also confirm the compatibility of the predicted outputs, in which the relative error is mainly around 0.2% and reaches a maximum of 0.5% at some points. Moreover, the simplified simulation model's computational cost for a long-term thermal performance prediction of the PSC is considerably less than a FEM-based simulation model. The simulation run time of the presented simplified simulation model over the calendar year of 2018 was only 3 s (i.e., without one-time parametrization procedure), compared to approximately 22 hours to simulate the FEM model for only one month (300000 times faster).

A sensitivity analysis has been performed on different design parameters such as the pipe spacing, pipe embedment depth, flow rate, and asphalt conductivity to identify and confirm the influence of these parameters on system performance. The sensitivity analysis also provides an overview of the parameter variation of the heat transfer coefficient UA^* and correlation parameter k in different PSC configurations. It is shown that the efficiency index (in the wintertime) enhances with an increase in pipe spacing, pipe embedment depth, and flow rate. However, an increase in the asphalt thermal conductivity decreases the efficiency index. These outcomes of the sensitivity analysis are confirmed by various studies in the literature.

The major limitation of the presented model is that it is not able to model a PSC system in detail (i.e., temperature distribution on surface or depth of asphalt pavement), and the model only provides an overview of the thermal performance of the system. Also, measurement or simulated data are necessary as input for the parametrization of the model. Finally, future studies need to be conducted to improve the model regarding parametrization using experimental data, integration into Simulink, and connection with other thermal models (e.g., heat pump and seasonal heat storage).

Author contributions

Taher Ghalandari: Methodology, Software, Validation, Writing- Original draft preparation. **David Ceulemans:** Conceptualization, Methodology, Software, Writing- Reviewing and Editing. **Navid Hasheminejad:** Writing- Reviewing and Editing. **Gert Guldentops:** Software, Validation. **Wim Van den bergh:** Supervision, Funding acquisition. **Ivan Verhaert:** Conceptualization, Writing- Reviewing and

Editing, Funding acquisition. **Cedric Vuye:** Writing- Reviewing and Editing, Methodology, Supervision, Funding acquisition.

Acknowledgments

This research did not receive any form of funding from public agencies, commercial, or not-for-profit sectors. The first author would like to acknowledge the University of Antwerp for the doctoral funding.

References

1. Pei, J., B. Zhou, and L. Lyu, *e-Road: The largest energy supply of the future?* Applied Energy, 2019. **241**: p. 174-183.
2. Ahmad, S., M. Abdul Mujeebu, and M.A. Farooqi, *Energy harvesting from pavements and roadways: A comprehensive review of technologies, materials, and challenges.* International Journal of Energy Research, 2019. **43**(6): p. 1974-2015.
3. Concha, J.L. and J. Norambuena-Contreras, *Thermophysical properties and heating performance of self-healing asphalt mixture with fibres and its application as a solar collector.* Applied Thermal Engineering, 2020. **178**: p. 115632.
4. Asfour, S., et al., *Hydrothermal modeling of porous pavement for its surface de-freezing.* Applied Thermal Engineering, 2016. **107**: p. 493-500.
5. Mallick, R.B., B.-L. Chen, and S. Bhowmick, *Harvesting heat energy from asphalt pavements: development of and comparison between numerical models and experiment.* International Journal of Sustainable Engineering, 2012. **5**(2): p. 159-169.
6. Mallick, R.B., B.-L. Chen, and S. Bhowmick, *Harvesting energy from asphalt pavements and reducing the heat island effect.* International Journal of Sustainable Engineering, 2009. **2**(3): p. 214-228.
7. Yu, X., A.J. Puppala, and N. Zhang, *Use of geothermal energy for deicing approach pavement slabs and bridge decks, phase 1*. 2017, Texas. Dept. of Transportation. Research and Technology Implementation Office.
8. Mirzanamadi, R., et al., *Anti-icing of road surfaces using Hydronic Heating Pavement with low temperature.* Cold Regions Science and Technology, 2018. **145**: p. 106-118.
9. Mirzanamadi, R., C.-E. Hagentoft, and P. Johansson, *Coupling a Hydronic Heating Pavement to a Horizontal Ground Heat Exchanger for harvesting solar energy and heating road surfaces.* Renewable Energy, 2020. **147**: p. 447-463.
10. Chen, J., H. Wang, and H. Zhu, *Analytical approach for evaluating temperature field of thermal modified asphalt pavement and urban heat island effect.* Applied Thermal Engineering, 2017. **113**: p. 739-748.
11. Ghalandari, T., et al., *A critical review on large-scale research prototypes and actual projects of hydronic asphalt pavement systems.* Renewable Energy, 2021. **177**: p. 1421-1437.
12. Alonso-Estébanez, A., et al., *3D numerical modelling and experimental validation of an asphalt solar collector.* Applied Thermal Engineering, 2017. **126**: p. 678-688.
13. Shaopeng, W., C. Mingyu, and Z. Jizhe, *Laboratory investigation into thermal response of asphalt pavements as solar collector by application of small-scale slabs.* Applied Thermal Engineering, 2011. **31**(10): p. 1582-1587.
14. Johnsson, J. and B. Adl-Zarrabi, *A numerical and experimental study of a pavement solar collector for the northern hemisphere.* Applied Energy, 2020. **260**: p. 114286.
15. Saleh, N.F., et al., *Design, construction, and evaluation of energy-harvesting asphalt pavement systems.* Road Materials and Pavement Design, 2019: p. 1-28.

16. Loomans, M., et al. *Design tool for the thermal energy potential of asphalt pavements*. in *Eighth International IBPSA Conference, Eindhoven, Netherlands*. 2003.
17. Liu, X., *Development and experimental validation of simulation of hydronic snow melting systems for bridges*. 2005, Oklahoma State University.
18. Guldentops, G., et al., *Performance of a pavement solar energy collector: Model development and validation.* Applied Energy, 2016. **163**: p. 180-189.
19. Mirzanamadi, R., C.-E. Hagentoft, and P. Johansson, *An analysis of hydronic heating pavement to optimize the required energy for anti-icing.* Applied Thermal Engineering, 2018. **144**: p. 278-290.
20. Masoumi, A.P., E. Tajalli-Ardekani, and A.A. Golneshan, *Investigation on performance of an asphalt solar collector: CFD analysis, experimental validation and neural network modeling.* Solar Energy, 2020. **207**: p. 703-719.
21. Zaim, E.H., H. Farzan, and M. Ameri, *Assessment of pipe configurations on heat dynamics and performance of pavement solar collectors: An experimental and numerical study.* Sustainable Energy Technologies and Assessments, 2020. **37**: p. 100635.
22. Van Riet Freek, V.R., C. Jonas, and V. Ivan. *Hydronic Optimization of Hybrid Heat Production Systems: a Methodology Based on Base Circuits*. in *Proceedings of Building Simulation*. 2019.
23. Van Riet, F. and I. Verhaert, *Hydronic configurations of hybrid heat production systems in buildings: General design methodology and case studies.* Applied Thermal Engineering, 2020. **164**: p. 114454.
24. Dakessian, L., et al., *Finite element approach to assess the benefits of asphalt solar collectors.* Transportation Research Record, 2016. **2575**(1): p. 79-91.
25. Bobes-Jesus, V., et al., *Asphalt solar collectors: a literature review.* Applied Energy, 2013. **102**: p. 962-970.
26. Guldentops, G., *Analysis of an Asphalt Pavement Solar Collector Using a Finite Element Approach*. 2014, Universiteit Antwerpen. p. 171.
27. Qin, Y. and J.E. Hiller, *Modeling temperature distribution in rigid pavement slabs: Impact of air temperature.* Construction and Building Materials, 2011. **25**(9): p. 3753-3761.
28. Dawson, A.R., et al., *Enhancing thermal properties of asphalt materials for heat storage and transfer applications.* Road Materials and Pavement Design, 2012. **13**(4): p. 784-803.
29. Radioti, G., et al., *Effect of undisturbed ground temperature on the design of closed-loop geothermal systems: A case study in a semi-urban environment.* Applied Energy, 2017. **200**: p. 89-105.
30. Bergman, T.L., et al., *Fundamentals of heat and mass transfer*. 2011: John Wiley & Sons.
31. Ghalandari, T., et al., *The use of a large-scale prototype to investigate the actual performance of a Heat Exchanging Asphalt Layer (published online)*, in *7th Eurasphalt & Eurobitume Congress*. 2021: Madrid, Spain.
32. Baetens, R., et al. *The exploration of the use of a heat exchanging asphalt layer as a prosumer in a low temperature heating grid*. in *Proceedings of the REHVA Annual Meeting Conference, Low Carbon Technologies in HVAC*. Brussels, Belgium.
33. Jacobs, G., J. Blom, and L. Lauriks. *The use of thermal infrared line scanner as a qualitative tool for asphalt paving process: a case study*. in *Bituminous Mixtures and Pavements VII: Proceedings of the 7th International Conference'Bituminous Mixtures and Pavements'(7ICONFBMP), June 12-14, 2019, Thessaloniki, Greece/Nikolaides, AF [edit.]*. 2019.
34. Van den Bergh, W., et al. *Demonstrating Innovative Technologies for the Flemish Asphalt Sector in the CyPaTs Project*. 2019. IOP Publishing.
35. van Bijsterveld, W.T., et al., *Using Pavement as Solar Collector: Effect on Pavement Temperature and Structural Response.* Transportation Research Record, 2001. **1778**(1): p. 140-148.

36. Van Bijsterveld, W. and A. De Bondt. *Structural aspects of asphalt pavement heating and cooling systems*. in *Proc., 3rd Int. Symp. on 3D Finite Element Modelling, Design and Research*. 2002.

37. Pan, P., et al., *A review on hydronic asphalt pavement for energy harvesting and snow melting.* Renewable & Sustainable Energy Reviews, 2015. **48**: p. 624-634.